Disclinations in a homogeneously deformed nematic elastomer

Eliot Fried[*,**] & Bidhan C. Roy[*]
[*]Department of Mechanical Engineering
Washington University
Saint Louis, MO 63130, USA
[**]Department of Theoretical and Applied Mechanics
University of Illinois at Urbana-Champaign
Urbana, IL 61801-2935, USA

Abstract

We consider the question of whether a nematic elastomer cross-linked in an isotropic state and then subjected to an isochoric, homogenous deformation can exhibit a disclination. The theory that we use allows for the polymer chains that comprise the network to adopt spherical, uniaxial, or biaxial conformations. The conformation is represented in terms of an orthogonal pair of directors and an associated pair of asphericities. A disclination is a tubular region in which the asphericities vanish and the directors are undefined, so that the conformation is spherical and the material appears to be isotropic. We apply the theory to a cylindrical specimen with circular cross-section deformed so that each cross-section becomes an ellipse. Assuming that, when they exist, the directors are parallel to the level sets of the deformation, the governing equations of the theory reduce to a boundary-value problem involving a pair of semilinear elliptic partial-differential equations for the asphericities. Numerical solutions of that problem predict that the specimen can adopt states in which an isotropic tubular core with characteristic cross-section on the order of 10^{-2} μm is surrounded by material in which the conformation is biaxial. Energetic considerations show that, for reasonable choices of the material parameters, such states are preferred for strains greater than or equal to 0.7% and thus are very likely to be observed. The theory also predicts that the transition between the undistorted isotropic reference state and the biaxial disclinated state is of second order.

Keywords: nematic elastomers; disclinations; biaxiality; energy minimizing states

1 Introduction

A nematic elastomer is a rubber-like solid formed by cross-linking a polymeric fluid that includes liquid–crystalline molecules as elements of its main chain and/or as pendant side groups. Like nematic liquid crystals, such materials possess local orientational order but lack the long–range translational order of crystalline solids.

Recently, Fried and Todres[1,2] considered the question of whether a nematic-elastomeric specimen subjected to inhomogeneous deformations involving an isochoric combination of radial and axial distortions can sustain disclinations. In that work, it was assumed that the material was cross-linked in an uniaxial state and subsequently annealed to create an isotropic reference state. Furthermore, the molecular conformation was restricted to be either spherical or uniaxial. Fried and Todres found that, even for mild distortions of the specimen, the material exhibits an energetic preference for states in which the molecular conformation is uniaxial except within a cylindrical core, surrounding the axis of the specimen, where the molecular conformation is spherical. That core region, which has characteristic dimension 10^{-2} μm, is identified as a disclination. As an extension of previous work, Fried, Korchagin and Todres[3] explored the possibile existence states in the conformation in the extra-core

region is biaxial. Their results indicate a strong energetic preference for such states over alternative states in which the conformation within the extra-core region is uniaxial.

Here, we address the question of whether a nematic-elastomeric specimen cross-linked in an *isotropic* state and then subjected to an isochoric, *homogeneous* deformation can sustain energetically preferred states involving disclinations. Because of the relative ease of producing isotropic specimens and the simplicity of homogenous deformations, these choices should facilitate experimental validation of theorical predictions.

To achieve this, we employ a framework developed by Fried, Korchagin and Todres.[3] That framework allows for the polymer chains that comprise the network to adopt spherical, uniaxial, or biaxial conformations. The conformation is represented in terms of an orthogonal pair of unit directors and an associated pair of asphericities. A disclination is then a tubular neighborhood about a space curve within which the asphericities vanish and the directors are undefined. Within a disclinated zone, the conformation is spherical and the material appears to be isotropic.

We consider a cylindrical specimen with circular cross-section and investigate the response of that specimen to deformations under which each undeformed cross-section is transformed homogeneously into an ellipse while preserving area locally. Assuming that, where they exist, the directors are parallel to the level sets of the deformation, the governing equations of the theory reduce to a boundary-value problem involving a pair of semilinear elliptic partial-differential equations for the asphericities which determine the conformation. We use numerical methods to obtain solutions to that system subject to variationally-natural boundary conditions, with the objective of determining whether the isochoric, homogeneous deformation of a specimen cross-linked in an isotropic state can generate disclinations.

2 Theory

The kinematic description of a nematic elastomer involves two fields: the vector-valued deformation $\boldsymbol{y}$ and the symmetric, positive-definite, tensor-valued, molecular conformation $\boldsymbol{A}$. Associated with $\boldsymbol{y}$ is the deformation-gradient $\boldsymbol{F}$, which serves as a macroscopic measure of the distortion of the polymer network. Assuming that the medium is incompressible, we must have $\det \boldsymbol{F} = 1$. The molecular conformation is a macroscopic measure of the nematically-induced distortion of the polymer chains that comprise the network. Being symmetric and positive-definite, $\boldsymbol{A}$ may be spherical, uniaxial, or biaxial. When $\boldsymbol{A}$ is spherical, the medium behaves as conventional isotropic rubber. Otherwise, the optical-mechanical behavior of the material is anisotropic. In general, we may represent $\boldsymbol{A}$ in the form

$$\boldsymbol{A} = a(1+q_1)^{-\frac{1}{3}}(1+q_2)^{-\frac{1}{3}}(\boldsymbol{1} + q_1\boldsymbol{n}_1\otimes\boldsymbol{n}_1 + q_2\boldsymbol{n}_2\otimes\boldsymbol{n}_2), \tag{1}$$

with $a = \det \boldsymbol{A} > 0$, $q_1 > -1$ and $q_2 > -1$ scalar asphericities, and $\boldsymbol{n}_1$ and $\boldsymbol{n}_2$ orthogonal ($\boldsymbol{n}_1\cdot\boldsymbol{n}_2 = 0$), unit ($|\boldsymbol{n}_\beta| = 1$, $\beta = 1, 2$) directors. The polymer chains are oblate, spherical, or prolate about $\boldsymbol{n}_\beta$ according to whether $-1 < q_\beta < 0$, $q_\beta = 0$, or $q_\beta > 0$.

We restrict attention to a nematic elastomer that is cross-linked in an isotropic state. In view of the representation (1), the net free-energy density should vary with $\boldsymbol{F}$, q_1, q_2, $\boldsymbol{n}_1$, and $\boldsymbol{n}_2$. To account for energetic contributions associated with conformational inhomogeneities, we allow also for dependence on the gradients $\boldsymbol{h}_1 = \operatorname{Grad} q_1$, $\boldsymbol{h}_2 = \operatorname{Grad} q_2$, $\boldsymbol{G}_1 = \operatorname{Grad} \boldsymbol{n}_1$, and $\boldsymbol{G}_2 = \operatorname{Grad} \boldsymbol{n}_2$ of the asphericies and directors. To be definite, we work with the particular free-energy density

$$\begin{aligned}\psi = \frac{\mu}{2}\Big((1+q_1)^{\frac{1}{3}}(1+q_2)^{\frac{1}{3}}\Big(|\boldsymbol{F}|^2 - \frac{q_1}{1+q_1}|\boldsymbol{F}^\top\boldsymbol{n}_1|^2 - \frac{q_2}{1+q_2}|\boldsymbol{F}^\top\boldsymbol{n}_2|^2\Big) - 3\Big) \\ + \Phi(q_1, q_2) + \frac{\alpha}{2}|\boldsymbol{h}_1|^2 + \frac{\alpha}{2}|\boldsymbol{h}_2|^2 + \Gamma(q_1)K(\boldsymbol{F}, \boldsymbol{n}_1, \boldsymbol{G}_1) + \Gamma(q_2)K(\boldsymbol{F}, \boldsymbol{n}_2, \boldsymbol{G}_2).\end{aligned} \tag{2}$$

The first term on the right side of (2) is the neo-classical free-energy density $\frac{1}{2}\mu(\operatorname{tr}(\boldsymbol{A}^{-1}\boldsymbol{F}\boldsymbol{\Lambda}\boldsymbol{F}^\top) - \ln\det(\boldsymbol{A}^{-1}\boldsymbol{\Lambda}) - 3)$ of Warner, Blandon and Terentjev[4] specialized to the case where conformation $\boldsymbol{\Lambda}$ at

the instant of cross-linking is isotropic ($\boldsymbol{\Lambda} = a\boldsymbol{1}$) and rewritten in terms of the explicit representation (1) for $\boldsymbol{A}$. Here, $\mu > 0$ is the shear modulus.

The second term on the right side of (2) is a potential that penalizes deviations of the asphericities q_1 and q_2 from the referentially preferred isotropic values $q_1 = 0$ and $q_2 = 0$. Accordingly, the potential Φ should be convex obey

$$\Phi(0,0) < \Phi(q_1, q_2) \qquad \text{if } q_1 \neq 0 \text{ or } q_2 \neq 0. \tag{3}$$

Consistent with the notion that overly oblate or prolate conformations should be energetically costly, we assume that Φ obeys

$$\Phi(q_1, q_2) \to +\infty \quad \text{as } q_1 \to -1, +\infty \text{ or } q_2 \to -1, +\infty. \tag{4}$$

Further, motivated by the observation that the expression (1) determining $\boldsymbol{A}$ in terms of q_1, $\boldsymbol{n}_1$, q_2, and $\boldsymbol{n}_2$ is invariant with respect to transformations of the form $\{(q_1, \boldsymbol{n}_1), (q_2, \boldsymbol{n}_2)\} \mapsto \{(q_2, \boldsymbol{n}_2), (q_1, \boldsymbol{n}_1)\}$, we assume that Φ is symmetric in the sense that

$$\Phi(q_1, q_2) = \Phi(q_2, q_1) \qquad \text{for all } (q_1, q_2). \tag{5}$$

The third and fourth terms on the right side of (2) are quadratic in the asphericity gradients $\boldsymbol{h}_1 = \operatorname{Grad} q_1$ and $\boldsymbol{h}_2 = \operatorname{Grad} q_2$. These terms, which involve a single parameter $\alpha > 0$ that might be referred to as an asperical elasticity modulus, penalize spatial inhomogeneities of the asphericities.

The last two terms on the right side of (2) are generalizations of the free-energy density arising in the Oseen–Zöcher–Frank theory for uniaxial nematic liquid crystals.[2] The factor K appearing in both of these terms has the particular form

$$\begin{aligned} K(\boldsymbol{F}, \boldsymbol{n}, \boldsymbol{G}) = \frac{\kappa_1}{2}(\boldsymbol{F}\cdot\boldsymbol{G})^2 + \frac{\kappa_2}{2}|\boldsymbol{F}^\top\boldsymbol{G}|^2 + \frac{\kappa_3(|\boldsymbol{F}^\top\boldsymbol{G}\boldsymbol{F}^\top\boldsymbol{n}|^2 + |\boldsymbol{G}^\top\boldsymbol{F}\boldsymbol{F}^\top\boldsymbol{n}|^2)}{2|\boldsymbol{F}^\top\boldsymbol{n}|^2} \\ + \frac{\kappa_4}{2}(\boldsymbol{F}^\top\boldsymbol{G})\cdot(\boldsymbol{G}^\top\boldsymbol{F}) + \frac{\kappa_5(\boldsymbol{F}^\top\boldsymbol{G}\boldsymbol{F}^\top\boldsymbol{n})\cdot(\boldsymbol{G}^\top\boldsymbol{F}\boldsymbol{F}^\top\boldsymbol{n})}{2|\boldsymbol{F}^\top\boldsymbol{n}|^2}. \end{aligned} \tag{6}$$

On setting $\boldsymbol{F} = \boldsymbol{1}$ in (6), we may identify $\kappa_1 + \kappa_2 + \kappa_4$, κ_2, $\kappa_2 + \kappa_3$, and $\kappa_2 + \kappa_4$ with the classical splay, twist, bend, and saddle-splay moduli of the Oseen–Zöcher–Frank theory; $\kappa_3 + \kappa_5$ is an additional modulus that accounts for interactions between the distortion of the network and the orientation of the molecular conformation as described by the directors $\boldsymbol{n}_1$ and $\boldsymbol{n}_2$. The remaining factor appearing in the last two terms on the right side of (2) mollifies singularities that accompany disclinations. Like Fried and Todres[2] and Fried, Korchagin and Todres,[3] we view a disclination in a nematic elastomer is a tubular region within which the asphericities vanish and the directors are undefined. When a director is undefined, its gradient is singular. Hence, the associated quantity K is also singular. The molifying factor Γ of the final, two terms on the right side of (2) render any such singularities integrable.[5] As such, Γ should obey

$$\left.\begin{aligned} \Gamma(q) = O(q_\beta^2) \quad \text{as } q \to 0, \\ \Gamma(q) > 0 \quad \text{for } q \neq 0, \\ \Gamma(q) \to +\infty \quad \text{as } q \to -1, +\infty. \end{aligned}\right\} \tag{7}$$

If we restrict attention to states in which the asphericity is uniaxial, so that, without loss of generality, $q_1 \equiv q \neq 0$ and $q_2 \equiv 0$, then the free-energy density (2) resembles the expression used by Fried, Korchagin and Todres,[3] the difference being in the properties of the potential Φ. Here, because we consider a material that is cross-linked directly in an isotropic state, Φ has only a single well. In contrast, Fried, Korchagin and Todres[3] use a multiwelled potential that embodies energetic

preferences for a uniaxial state present at the time of cross-linking and an isotropic reference state obtained subsequently by annealing.

As a consequence of the dependence of the free-energy density (2) on the variables $\boldsymbol{F}$, q_1, q_2, $\boldsymbol{h}_1 = \mathrm{Grad}\, q_1$, $\boldsymbol{h}_2 = \mathrm{Grad}\, q_2$, $\boldsymbol{n}_1$, $\boldsymbol{n}_2$, $\boldsymbol{G}_1 = \mathrm{Grad}\, \boldsymbol{n}_1$, and $\boldsymbol{G}_2 = \mathrm{Grad}\, \boldsymbol{n}_2$, the theory gives rise to the following variationally-based equilibrium equations:

$$\left.\begin{aligned} \mathrm{Div}\Big(\frac{\partial \psi}{\partial \boldsymbol{F}}\Big) &= \boldsymbol{F}^{-\top}\mathrm{Grad}\, p, \\ \mathrm{Div}\Big(\frac{\partial \psi}{\partial \boldsymbol{h}_1}\Big) &= \frac{\partial \psi}{\partial q_1}, \\ \mathrm{Div}\Big(\frac{\partial \psi}{\partial \boldsymbol{h}_2}\Big) &= \frac{\partial \psi}{\partial q_2}, \\ \mathrm{Div}\Big(\frac{\partial \psi}{\partial \boldsymbol{G}_1}\Big) + \Big(\frac{\partial \psi}{\partial \boldsymbol{G}_1}\cdot \boldsymbol{G}_1\Big)\boldsymbol{n}_1 &= \frac{\partial \psi}{\partial \boldsymbol{n}_1}, \\ \mathrm{Div}\Big(\frac{\partial \psi}{\partial \boldsymbol{G}_2}\Big) + \Big(\frac{\partial \psi}{\partial \boldsymbol{G}_2}\cdot \boldsymbol{G}_2\Big)\boldsymbol{n}_2 &= \frac{\partial \psi}{\partial \boldsymbol{n}_2}. \end{aligned}\right\} \tag{8}$$

Here, all differentiation of ψ is performed on the manifold associated with the constraints $\det \boldsymbol{F} = 1$, $|\boldsymbol{n}_1| = 1$, and $|\boldsymbol{n}_2| = 1$. In particular, p denotes the pressure required to maintain the first of these constraints. While $(8)_1$ expresses the conventional force balance associated with $\boldsymbol{y}$, $(8)_2$, $(8)_3$, $(8)_4$, and $(8)_5$ express generalized force balances associated, respectively, with the additional kinematical degrees of freedom q_1, q_2, $\boldsymbol{n}_1$, and $\boldsymbol{n}_2$.

Consider a specimen that occupies a region $\mathcal{R}$. For a subset $\mathcal{S}$ of the boundary $\partial\mathcal{R}$ of $\mathcal{R}$ with unit outward normal $\boldsymbol{\nu}$, variationally-based natural boundary conditions to accompany the governing equations (8) are:

$$\left.\begin{aligned} \Big(\frac{\partial \psi}{\partial \boldsymbol{F}} - p\boldsymbol{F}^{-\top}\Big)\Big|_{\partial\mathcal{R}}\boldsymbol{\nu} &= \boldsymbol{0}, \\ \frac{\partial \psi}{\partial \boldsymbol{h}_1}\Big|_{\partial\mathcal{R}}\cdot\boldsymbol{\nu} &= 0, \\ \frac{\partial \psi}{\partial \boldsymbol{h}_2}\Big|_{\partial\mathcal{R}}\cdot\boldsymbol{\nu} &= 0, \\ \frac{\partial \psi}{\partial \boldsymbol{G}_1}\Big|_{\partial\mathcal{R}}\boldsymbol{\nu} &= \boldsymbol{0}, \\ \frac{\partial \psi}{\partial \boldsymbol{G}_2}\Big|_{\partial\mathcal{R}}\boldsymbol{\nu} &= \boldsymbol{0}. \end{aligned}\right\} \tag{9}$$

While $(9)_1$ expresses the requirement that $\mathcal{S}$ be traction-free in the standard sense, $(9)_2$, $(9)_3$, $(9)_4$, and $(9)_5$ express the requirment that $\mathcal{S}$ be free of the generalized tractions associated with q_1, q_2, $\boldsymbol{n}_1$, and $\boldsymbol{n}_2$.

3 Application

We now apply the theory to study the deformation of a cylindrical specimen with circular cross-section. Specifically, we choose a fixed orthonormal basis $\{\boldsymbol{e}_1, \boldsymbol{e}_2, \boldsymbol{e}_3\}$ and consider a reference state in which the medium occupies the cylindrical region

$$\mathcal{R} = \{\boldsymbol{x} : \sqrt{{x_1}^2 + {x_2}^2} \leq R, -\infty < x_3 < \infty\},$$

with $x_i = \boldsymbol{x}\cdot\boldsymbol{e}_i$. We introduce cylindrical-polar coordinates (r, θ, z) via

$$R = \sqrt{{x_1}^2 + {x_2}^2}, \qquad \theta = \arctan(x_2/x_1), \qquad z = x_3,$$

and let $\{\boldsymbol{e}_r, \boldsymbol{e}_\theta, \boldsymbol{e}_z\}$ denote the associated physical basis.

We assume that the lateral surface of the specimen is free of all tractions. Thus, the natural boundary conditions (9) hold with $\mathcal{S} = \{\boldsymbol{x} : |\boldsymbol{x}| = R\}$ and $\boldsymbol{\nu} = \boldsymbol{e}_r$.

We suppose that the specimen is subjected to the particular deformation

$$\boldsymbol{y}(r, \theta, z) = \lambda x_1 \boldsymbol{e}_1 + \frac{x_2}{\lambda}\boldsymbol{e}_2 + x_3 \boldsymbol{e}_3, \qquad \text{with} \quad \lambda \geq 1. \tag{10}$$

The deformation gradient is then homogeneous and of the form

$$\boldsymbol{F} = \lambda \boldsymbol{e}_1 \otimes \boldsymbol{e}_1 + \frac{1}{\lambda}\boldsymbol{e}_2 \otimes \boldsymbol{e}_2 + \boldsymbol{e}_3 \otimes \boldsymbol{e}_3. \tag{11}$$

Further, a direct calculation shows that $\det \boldsymbol{F} = 1$ holds throughout $\mathcal{R}$; thus, the assumed deformation is isochoric. Under a deformation of the form (10), each circular cross-section of the cylinder $\mathcal{R}$ is transformed into an ellipse with major and minor axes λR and R/λ.

Further, we assume that the asphericities are independent of z, viz.,

$$q_\beta(r, \theta, z) = q_\beta(r, \theta), \qquad \beta = 1, 2. \tag{12}$$

Except where the material is isotropic and $\boldsymbol{n}_1$ and $\boldsymbol{n}_2$ are undefined, we assume that

$$\left.\begin{aligned} \boldsymbol{n}_1 &= \frac{\cos^2\theta + \lambda^2 \sin^2\theta}{\sqrt{\cos^2\theta + \lambda^4 \sin^2\theta}}\boldsymbol{e}_r + \frac{(\lambda^2 - 1)\sin\theta\cos\theta}{\sqrt{\cos^2\theta + \lambda^4 \sin^2\theta}}\boldsymbol{e}_\theta, \\ \boldsymbol{n}_2 &= \frac{\cos^2\theta + \lambda^2 \sin^2\theta}{\sqrt{\cos^2\theta + \lambda^4 \sin^2\theta}}\boldsymbol{e}_\theta - \frac{(\lambda^2 - 1)\sin\theta\cos\theta}{\sqrt{\cos^2\theta + \lambda^4 \sin^2\theta}}\boldsymbol{e}_r. \end{aligned}\right\} \tag{13}$$

As a consequence of these choices, the constraints $|\boldsymbol{n}_1| = 1$ and $|\boldsymbol{n}_2| = 1$ are satisfied whenever $\boldsymbol{n}_1$ and $\boldsymbol{n}_2$ are defined. Where they exist, the directors are therefore perpendicular and parallel to the level sets of deformation. Most importantly, $\boldsymbol{n}_1$ and $\boldsymbol{n}_2$ as given are undefined on the axis of the specimen. A state corresponding to these choices then involves a disclination of strength $+1$ about the axis of the specimen. The combined ansatz embodied by (10) and (13) therefore allows us to consider whether the governing equations of the theory admit solutions and, moreover, whether such solutions are energetically feasible—that is, preferred for certain values of λ.

A direct calculation shows that, when $\boldsymbol{n}_1$ and $\boldsymbol{n}_2$ are defined,

$$\left.\begin{aligned} \boldsymbol{G}_1(r, \theta, z) &= \frac{\lambda^2(\cos^2\theta + \lambda^2 \sin^2\theta)}{r(\cos^2\theta + \lambda^4 \sin^2\theta)^{\frac{3}{2}}}\boldsymbol{e}_\theta \otimes \boldsymbol{e}_\theta - \frac{\lambda^2(\lambda^2 - 1)\sin\theta\cos\theta}{r(\cos^2\theta + \lambda^4 \sin^2\theta)^{\frac{3}{2}}}\boldsymbol{e}_r \otimes \boldsymbol{e}_\theta, \\ \boldsymbol{G}_2(r, \theta, z) &= \frac{\lambda^2(\cos^2\theta + \lambda^2 \sin^2\theta)}{r(\cos^2\theta + \lambda^4 \sin^2\theta)^{\frac{3}{2}}}\boldsymbol{e}_r \otimes \boldsymbol{e}_\theta - \frac{\lambda^2(\lambda^2 - 1)\sin\theta\cos\theta}{r(\cos^2\theta + \lambda^4 \sin^2\theta)^{\frac{3}{2}}}\boldsymbol{e}_\theta \otimes \boldsymbol{e}_\theta. \end{aligned}\right\} \tag{14}$$

Using (11)–(14) in (6) gives

$$\left.\begin{aligned} K(\boldsymbol{F}, \boldsymbol{n}_1, \boldsymbol{G}_1) &= \frac{\lambda^2}{2r^2(\cos^2\theta + \lambda^4 \sin^2\theta)}\left(\kappa_s + \frac{\kappa_b(\lambda^4 - 1)^2 \sin^2\theta\cos^2\theta}{(\cos^2\theta + \lambda^4 \sin^2\theta)^2}\right), \\ K(\boldsymbol{F}, \boldsymbol{n}_2, \boldsymbol{G}_2) &= \frac{\lambda^6 \kappa_b}{2r^2(\cos^2\theta + \lambda^4 \sin^2\theta)^3}, \end{aligned}\right\} \tag{15}$$

where $\kappa_s = \kappa_1 + \kappa_2 + \kappa_4$ and $\kappa_b = \kappa_2 + \kappa_3$ denote, respectively, the splay and bend moduli. Hence, of the parameters κ_1, κ_2, κ_3, κ_4, and κ_5 entering the generalized Oseen–Zöcher–Frank expression (6), the assumed forms (11) and (13) for the deformation and directors ensure that only the splay and bend moduli are of importance.

Since the deformation is prescribed via (10) and the directors are either given as in (13) or undefined, the only unknowns are the pressure p and asphericities q_1 and q_2. Granted knowledge of q_1 and q_2, using (11)–(14) in the conventional force balance $(8)_1$ and corresponding boundary condition $(9)_1$ yields a relation that determines the pressure; like the deformation, the asphericities, and the directors, the pressure is independent of the axial coordinate. In view of (11)–(14), the bulk equations $(8)_{2,3}$ and corresponding boundary conditions $(9)_{2,3}$ yield a seminlinear elliptic boundary-value problem for the asphericities. Finally, granted (13), a lengthy calculation shows that $(10)_{4,5}$ and $(8)_{4,5}$ are satisified identically. Thus, the problem under consideration reduces to the study of the boundary-value problem for q_1 and q_2.

4 Scaling. Final governing equations

To extract information from the boundary-value problem for the asphericities, we introduce a dimensionless radial coordinate $x = r/R$ and define

$$Q_\beta(x,\theta) = q_\beta(Rx,\theta), \qquad \beta = 1,2. \tag{16}$$

Additionally, we introduce a parameter $\nu > 0$, with dimensions of energy per unit volume that measures the characteristic strength of the convex potential Φ. (For instance, ν might be defined by the Hessian of Φ evaluated at $(q_1,q_2) = (0,0)$, where, consistent with (3), Φ attains its sole minimum). Bearing in mind that the molifier Γ is dimensionless, a simple dimensional argument based on (2), (6), and (15), leads to the identification of four dimensionless groups

$$\mu^* = \frac{\mu}{\nu}, \qquad \alpha^* = \frac{\alpha}{R^2\nu}, \qquad \kappa_s^* = \frac{\kappa_s}{R^2\nu}, \qquad \text{and} \qquad \kappa_b^* = \frac{\kappa_b}{R^2\nu}. \tag{17}$$

Using the kinematical assumptions (10)–(13) in $(8)_2$ and $(8)_3$ and taking advantage of the foregoing scaling, we arrive at the dimensionless partial-differential equations

$$\begin{aligned}\frac{\alpha^*}{x}\frac{\partial}{\partial x}\left(x\frac{\partial Q_1}{\partial x}\right) + \frac{\alpha^*}{x^2}\frac{\partial^2 Q_1}{\partial\theta^2} &= \frac{\mu^*(1+Q_2)^{\frac{1}{2}}}{6(1+Q_1)^{\frac{2}{3}}}\left(\lambda^2+\frac{1}{\lambda^2}+1\right) - \frac{\mu^*(3+Q_1)(1+Q_2)^{\frac{1}{3}}\lambda^2}{6(1+Q_1)^{\frac{5}{3}}(\cos^2\theta+\lambda^4\sin^2\theta)}\\ &\quad - \frac{\mu^* Q_2(\cos^2\theta+\lambda^8\sin^2\theta)}{6(1+Q_1)^{\frac{2}{3}}(1+Q_2)^{\frac{2}{3}}\lambda^2(\cos^2\theta+\lambda^4\sin^2\theta)} + \frac{1}{\nu}\frac{\partial\Psi(Q_1,Q_2)}{\partial Q_1}\\ &\quad + \frac{\lambda^2\Gamma'(Q_1)}{2x^2(\cos^2\theta+\lambda^4\sin^2\theta)}\left(\kappa_s^* + \frac{\kappa_b^*(\lambda^4-1)^2\sin^2\theta\cos^2\theta}{(\cos^2\theta+\lambda^4\sin^2\theta)^2}\right)\end{aligned} \tag{18}$$

and

$$\begin{aligned}\frac{\alpha^*}{x}\frac{\partial}{\partial x}\left(x\frac{\partial Q_2}{\partial x}\right) + \frac{\alpha^*}{x^2}\frac{\partial^2 Q_2}{\partial\theta^2} &= \frac{\mu^*(1+Q_1)^{\frac{1}{3}}}{6(1+Q_2)^{\frac{2}{3}}}\left(\lambda^2+\frac{1}{\lambda^2}+1\right) - \frac{\mu^*(3+Q_2)(1+Q_1)^{\frac{1}{3}}(\cos^2\theta+\lambda^8\sin^2\theta)}{(1+Q_2)^{\frac{5}{3}}\lambda^2(\cos^2\theta+\lambda^4\sin^2\theta)}\\ &\quad - \frac{\mu^* Q_1\lambda^2}{6(1+Q_1)^{\frac{2}{3}}(1+Q_2)^{\frac{2}{3}}(\cos^2\theta+\lambda^4\sin^2\theta)} + \frac{1}{\nu}\frac{\partial\Psi(Q_1,Q_2)}{\partial Q_2} + \frac{\lambda^6\Gamma'(Q_2)\kappa_b^*}{2x^2(\cos^2\theta+\lambda^4\sin^2\theta)^3}\end{aligned} \tag{19}$$

for Q_1 and Q_2; similarly, the boundary conditions $(9)_2$ specialize to yield

$$\left.\frac{\partial Q_1}{\partial x}\right|_{x=1} = 0 \qquad \text{and} \qquad \left.\frac{\partial Q_2}{\partial x}\right|_{x=1} = 0. \tag{20}$$

5 Numerical results

The partial differential equations (18) and (19) involve functions Φ and Γ. In addition to being convex, Φ must obey the restrictions (3), (4), and (5); Γ is restricted by (7). Although many choices would satisfy these restrictions, for our numerical investigations we took

$$\Phi(q_1, q_2) = \frac{\nu q_1^4}{2(1+q_1)^2} + \frac{\nu q_2^4}{2(1+q_2)^2} \tag{21}$$

and, as in Fried and Todres,[2]

$$\Gamma(q) = \begin{cases} \dfrac{q^2}{(1+q)^2} & \text{if } -1 < q \leq 0, \\ q^2 & \text{if } q \geq 0. \end{cases} \tag{22}$$

We emphasize that the particular forms for (21) and (22) are pragmatically based. While defined piecewise, the particular choice (22) of Γ is twice continuously-differentiable.

For our simulations, we chose $\mu = 10^5$ J/m^3, $\nu = 10^6$ J/m^3, and $R = 1$ cm. Underlying the chosen value of ν is the notion that, whereas μ should scale like $k_B\theta$ per polymer chain, with k_B Boltzmann's constant and θ the absolute temperature, ν should scale like $k_B\theta$ per monomer. To attain the high extensibilities associated with rubber-like behavior requires upwards of 15–100 monomers per chain, whereby ν should exceed μ by at least an order of magnitude. For traditional nematics at temperatures in a wide range below the clearing temperature, the bend modulus κ_b is on the order of 10^{-12} J/m and is three-halves to twice the splay modulus κ_s.[6–9] The values of these moduli have not yet been determined for nematic elastomers, but, because of the rubbery nature of these materials, it seems reasonable to expect that the moduli would be at least an order of magnitude greater.[10] So, we took $\kappa_s = 10^{-11}$ J/m and $\kappa_b = 2 \times 10^{-11}$ J/m. The value of the splay modulus is also in line with values used in previous work.[1–3,10–11] With the expectation that the regularizing modulus should not exceed the splay modulus, we chose $\alpha = 10^{-11}$. As a result of the foregoing assumptions,

$$\mu^* = 10^{-1} \qquad \text{and} \qquad \kappa_s^* = \tfrac{1}{2}\kappa_b^* = \alpha^* = 10^{-13}. \tag{23}$$

A some larger and, thus, more realistic value of α would lead to smaller values of α^*, κ_s^*, κ_b^* and, thus, intensify the challenge of performing simulations.

We now present the results of numerical simulations performed using `FISHPAK`.[13]

5.1 The core radius

Figures 1–2 shows plots of Q_1 and Q_2 along the radial direction for θ taking values of 0, $\frac{\pi}{2}$, π, and $\frac{3\pi}{2}$. They show a sharp transition between isotropic ($Q_1 = Q_2 = 0$) and anisotropic ($Q_\beta \neq 0$, $\beta = 1, 2$) regions along the cylinder radius, thereby indicating the presence of a disclination. From Figures 1–2, the transition zone between the isotropic and anisotropic regions appears to be at $x \approx 10^{-6}$, which corresponds to a core with characteristic dimension on the order of 10^{-2} μm. This agrees with the predictions of Fried and Todres[1,2] and Fried, Korchagin and Todres,[3] and is of the same order as values observed for liquid-crystalline melts.[12]

The characteristic dimension of the core is more easily visualized using the contours of the asphericities, Q_1 and Q_2, in the deformed geometry. To exhibit the contours of asphericity, we employ the coordinate stretching

$$X = \lambda x^{\frac{1}{4}} \cos\theta, \qquad Y = \frac{y^{\frac{1}{4}} \sin\theta}{\lambda}. \tag{24}$$

Figure 3 shows the density and surface plots of the asphericities as functions of position in the deformed domain for $\lambda = 1.2$. The boundary of the core corresponds to the region where Q_1 (or Q_2)

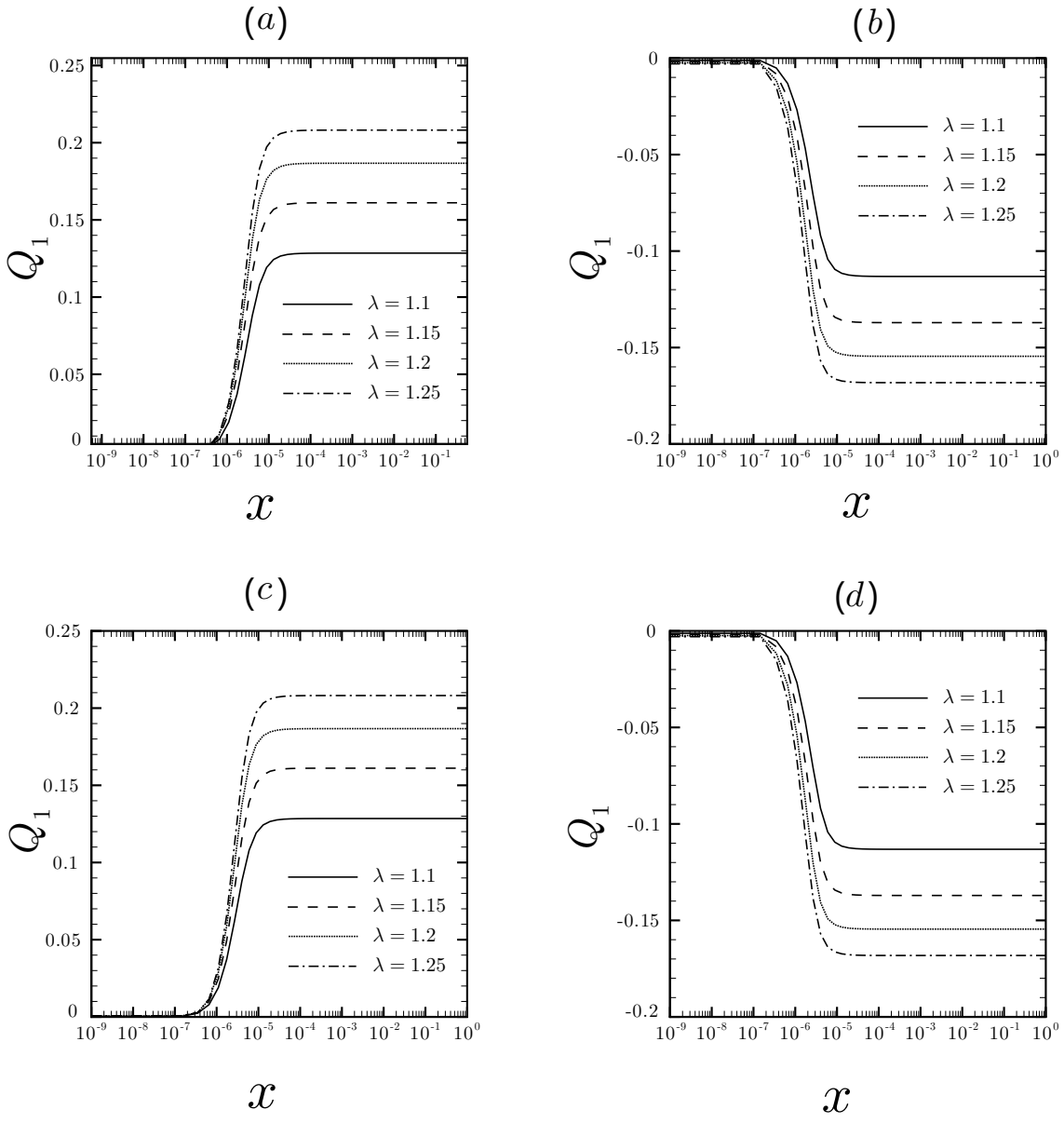

Figure 1: Plots of the asphericity Q_1 as a function of dimensionless radial position x (in log scale) for $\mu^* = 10^{-1}$, $\kappa_s^* = \alpha^* = 10^{-13}$, and $\kappa_b^* = 2 \times 10^{-13}$. Here: (a) $\theta = 0$; (b) $\theta = \frac{\pi}{2}$; (c) $\theta = \pi$; (d) $\theta = \frac{3\pi}{2}$.

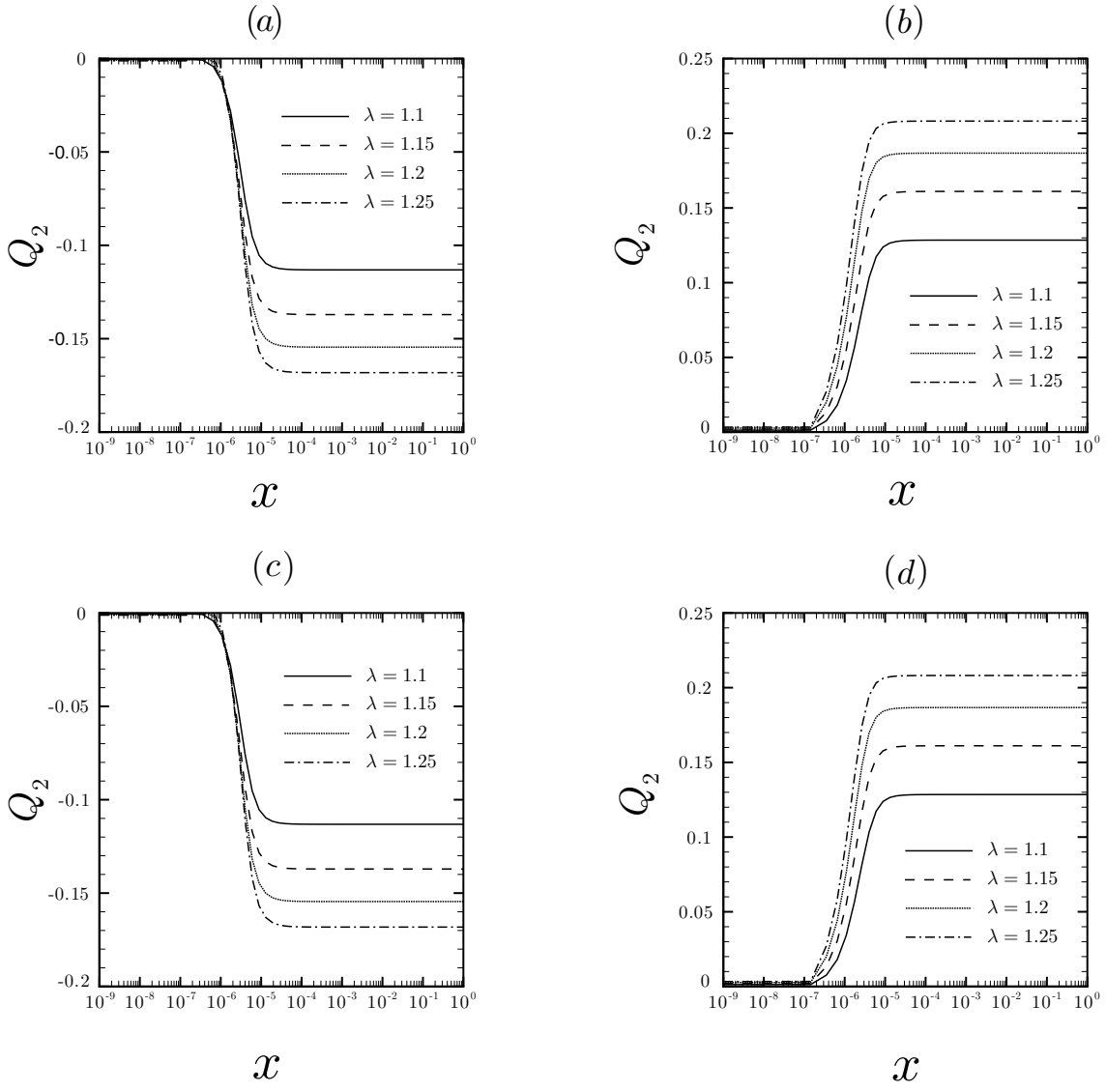

Figure 2: Plots of the asphericity Q_2 as a function of dimensionless radial position x (in log scale) for $\mu^* = 10^{-1}$, $\kappa_s^* = \alpha^* = 10^{-13}$, and $\kappa_b^* = 2 \times 10^{-13}$. Here: (a) $\theta = 0$; (b) $\theta = \frac{\pi}{2}$; (c) $\theta = \pi$; (d) $\theta = \frac{3\pi}{2}$.

Table 1: Comparison of the asphericities Q_1 and Q_2 with varying distortion λ

λ	$\max\limits_{\substack{0\le r\le 1\\ \theta=0,\pi}} Q_1(r,\theta)$	$\max\limits_{\substack{0\le r\le 1\\ \theta=\frac{\pi}{2},\frac{3\pi}{2}}} Q_1(r,\theta)$	$\min\limits_{\substack{0\le r\le 1\\ \theta=\frac{\pi}{2},\frac{3\pi}{2}}} Q_1(r,\theta)$	$\min\limits_{\substack{0\le r\le 1\\ \theta=0,\pi}} Q_1(r,\theta)$
1.1	0.1284	0.1293	-0.1131	-0.1131
1.15	0.1610	0.1626	-0.1370	-0.1370
1.2	0.1867	0.1963	-0.1545	-0.1545
1.25	0.2081	0.2081	-0.1681	-0.1681

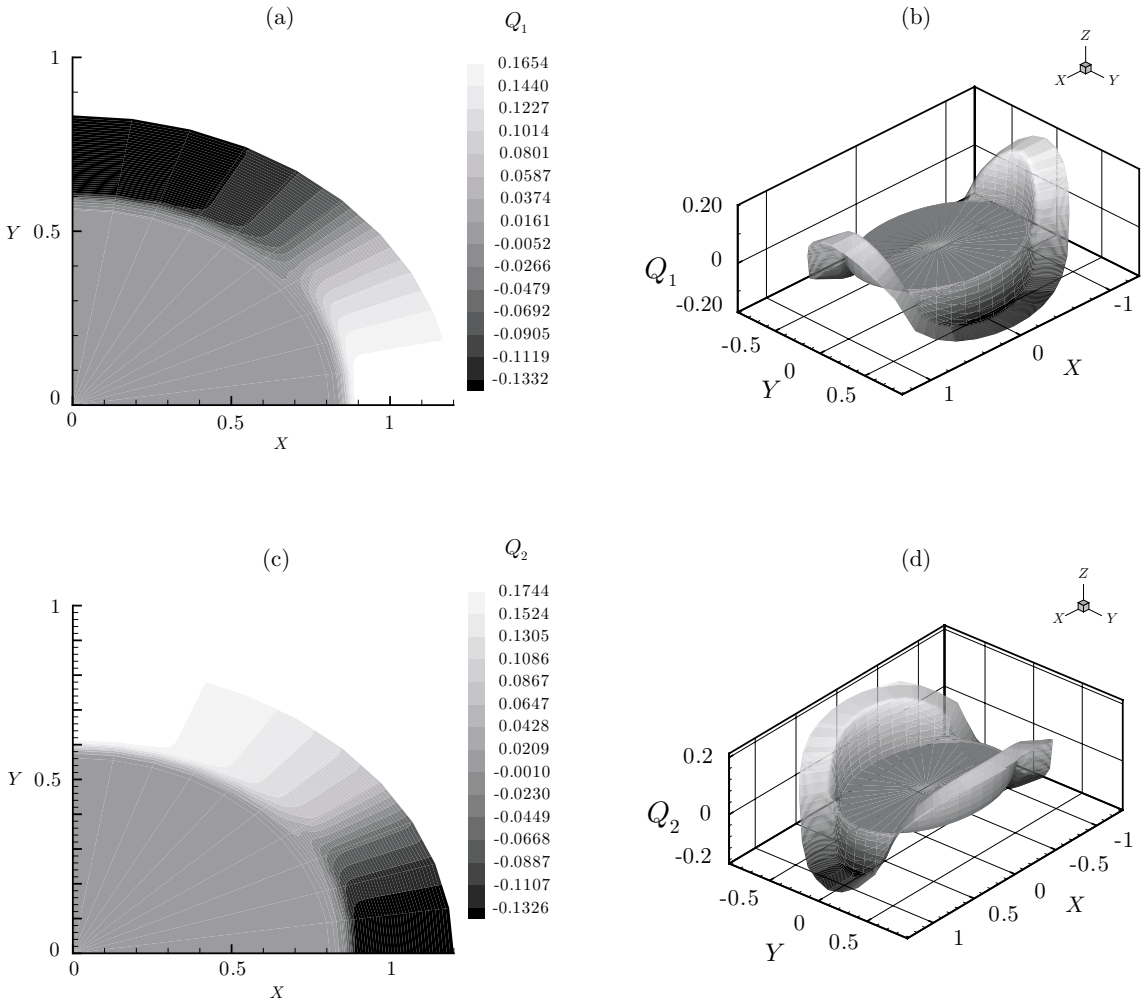

Figure 3: (a) Density plot of Q_1 in the deformed domain; (b) Surface plot of Q_1 in the deformed domain; (c) Density plot of Q_2 in the deformed domain; (d) Surface plot of Q_2 in the deformed domain. Here $\lambda = 1.1$, $\mu^* = 10^{-1}$, $\kappa_s^* = \alpha^* = 10^{-13}$, and $\kappa_b^* = 2 \times 10^{-13}$. All plots are for stretched coordinates $X = \lambda x^{\frac{1}{4}} \cos\theta$ and $Y = y^{\frac{1}{4}} \sin\theta/\lambda$.

increases or decreases rapidly to a nonzero value. Inside the disclination core, $Q_1 = Q_2 = 0$. Hence inside the disclination core the material is isotropic. Outside the disclination core, Q_1 and Q_2 both take non-trivial values. The states obtained numerically therefore involve *biaxial* conformations.

Table 1 compares the maximum and minimum values of Q_1 and Q_2 for various values of λ. The data indicates that Q_1 and Q_2 are out of phase by $\frac{\pi}{2}$, which is consistent with the orthogonality of the corresponding directors $\boldsymbol{n}_1 = \boldsymbol{e}_r$ and $\boldsymbol{n}_2 = \boldsymbol{e}_\theta$.

5.2 Energetic status of biaxial states

To investigate the energetic status of the numerically-determined biaxial disclinated states, we introduce the dimensionless free-energy density $\Psi = \psi/\nu$ and compare the dimensionless free-energy

$$\Psi^{\text{tot}} = \int_0^{2\pi} \int_0^1 \Psi(x,\theta) x \, \mathrm{d}x \, \mathrm{d}\theta \tag{25}$$

to the neo-Hookean energy

$$\Psi_e^{\text{tot}} = \frac{\mu^* \pi}{2} \left(\lambda^2 + \frac{1}{\lambda^2} - 2 \right). \tag{26}$$

Whereas Ψ^{tot} gives the free-energy of a generic cross-section for a biaxially disclinated specimen, Ψ_e^{tot} gives the free-energy of a comparison specimen that deforms like conventional rubber with neo-Hookean free-energy density $\mu(\text{tr}\,(\boldsymbol{F}\boldsymbol{F}^\top) - 3)$.

Using the computed values of Q_1 and Q_2, we calculate the total energy Ψ^{tot}. To determine whether our numerically determined disclinated states are energetically preferred, we plot both Ψ^{tot} and Ψ_e^{tot} (Figure 4). While Ψ_e^{tot} increases monotonically with λ, Ψ^{tot} has an inflection point at $\lambda \approx 1.007$. For $\lambda \leq 1.007$, Ψ^{tot} is slightly greater than Ψ_e^{tot}. However, for $\lambda \geq 1.007$, $\Psi^{\text{tot}} < \Psi_e^{\text{tot}}$. Thus, for strains in excess of the 0.7%, the material shows an energetic preference for a disclinated state.

Because the graph of Ψ^{tot} exhibits only a single minimum, the theory predicts that, for a specimen cross-linked in an isotropic state and then deformed in the homogenous manner considered here, the transition to a biaxially anisotropic disclinated state is of second order. This result stands in contrast to the results of Fried and Todres[2] and Fried, Korchagin and Todres,[3] who, for a cylindrical specimen cross-linked in a uniaxial state, annealed, and then subjected to isochoric radial expansion or contraction, observe a first-order transition between the isotropic reference state and an anisotropic disclinated state.

Denoting by

$$\Psi^{\text{core}} = \int_0^{2\pi} \int_0^{x_c} \Psi(x,\theta) x \, \mathrm{d}x \, \mathrm{d}\theta \tag{27}$$

the dimensionless free-energy of the core portion for any given cross-section of the specimen, we also considered the ratio $\Psi^{\text{core}}/\Psi^{\text{tot}}$, which gives the free-energy of the disclination core relative to that of the whole domain. From Figure 5, it is evident that Ψ^{core} is a vanishingly small percentage of Ψ^{tot}. This is because of the relatively small size of the core and the fact that Ψ_e is of a comparatively large magnitude across the entire radial extent of the cylinder. The proportion of total energy contained in the core remains relatively constant up to the value of λ corresponding to the inflection point of Ψ^{tot}. A sharp increase then occurs and continues monotonically until leveling off at $\lambda \approx 1.025$, at which stage the free-energy of the core remains fixed but more energy goes into stretching the network and altering the asphericity of the polymer chains in the extra-core region.

For a specimen deformed as described here, there is also the possibility that uniaxial disclinated states may exist. However, such states represent local energy minima and are, thus, unlikely to be observed. To illustrate this, Figure 6 shows plots of Ψ^{tot} and the total free-energy $\Psi_{\text{uni}}^{\text{tot}}$ corresponding to a disclinated state where theconformation in the extra-core region is uniaxial about the orientation

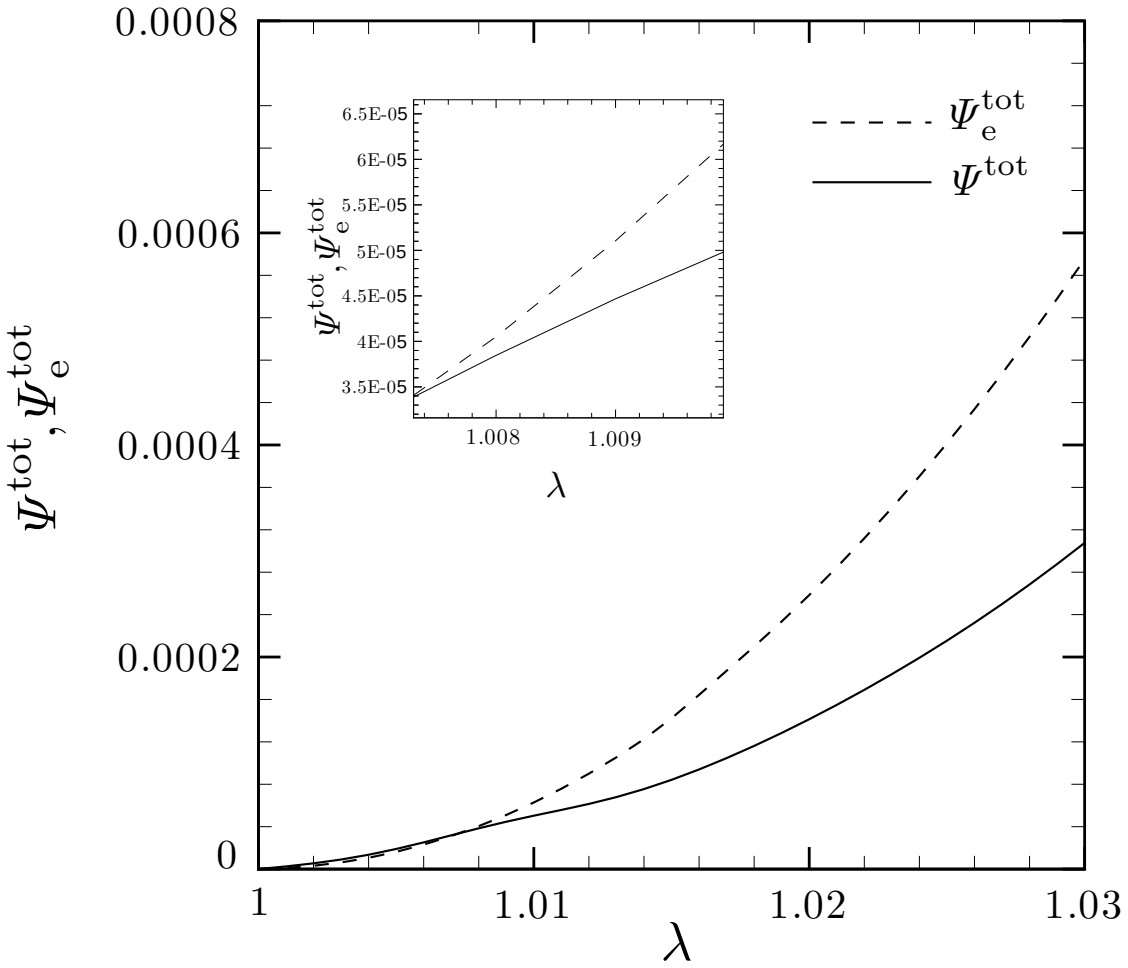

Figure 4: Comparison of neo-Hookean rubber-elastic energy $\Psi_e^{\rm tot}$ and the total free-energy $\Psi^{\rm tot}$. The figure in the inset is the region near the inflexion point. Here $\mu^* = 10^{-1}$, $\kappa_s^* = \alpha^* = 10^{-13}$, and $\kappa_b^* = 2 \times 10^{-13}$.

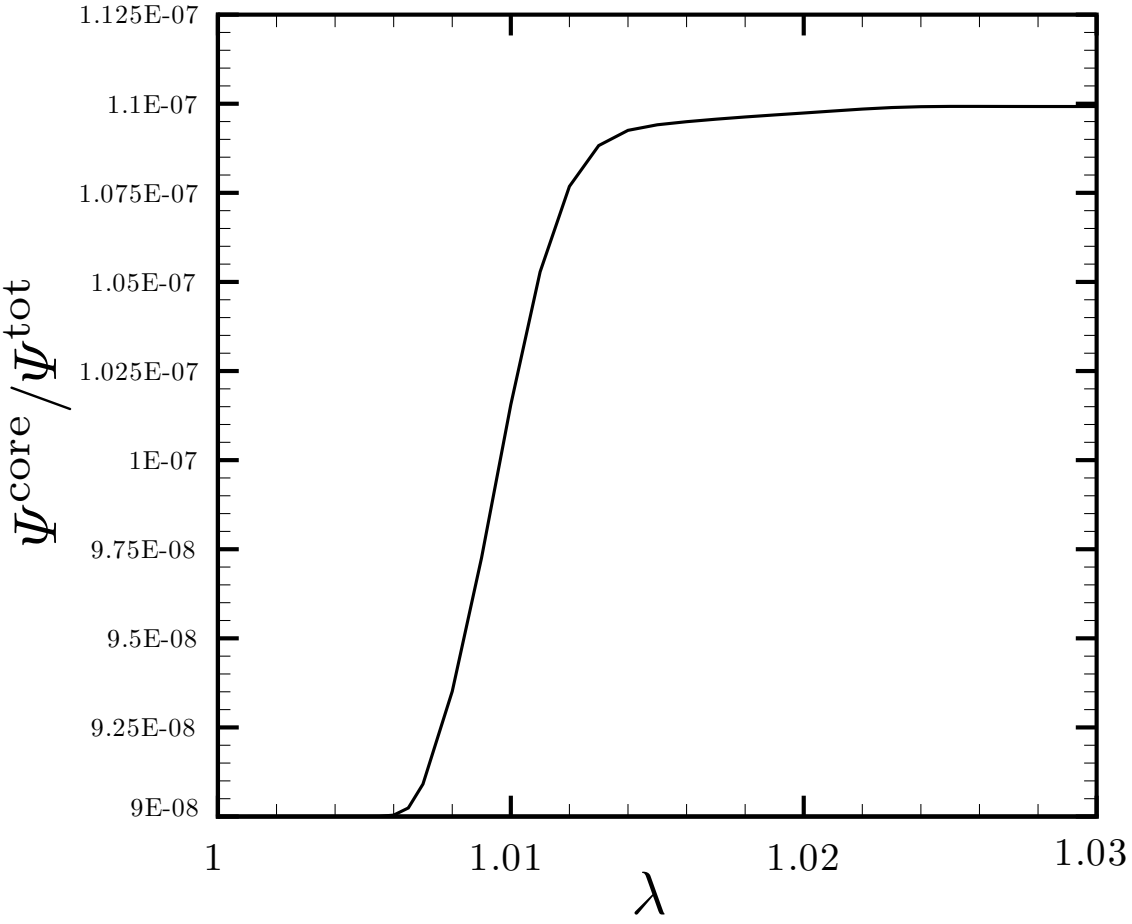

Figure 5: Plot of $\Psi^{\rm core}/\Psi^{\rm tot}$. Here $\mu^* = 10^{-1}$, $\kappa_s^* = \alpha^* = 10^{-13}$, and $\kappa_b^* = 2 \times 10^{-13}$.

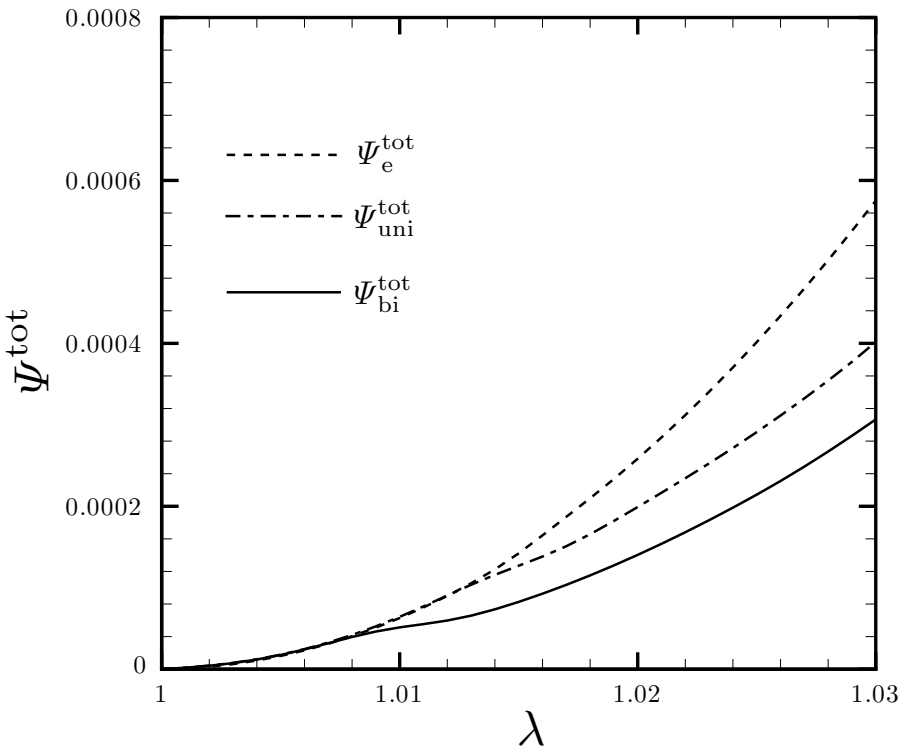

Figure 6: Comparison of neo-Hookean rubber-elastic energy $\Psi_e^{\rm tot}$, the total free-energy $\Psi^{\rm tot}$, and the total free-energy $\Psi^{\rm tot}_{\rm uni}$ when the orientation is in the radial direction. Here $\mu^* = 10^{-1}$, $\kappa_s^* = \alpha^* = 10^{-13}$, and $\kappa_b^* = 2 \times 10^{-13}$.

$\boldsymbol{n}_1$ as defined in $(13)_1$. From this plot it is clear that the transition between an isotropic state and a uniaxial disclinated state is, like the isotropic-biaxial transition, of second order. However, such a transition requires greater strain to be induced. Most importantly, $\Psi^{\rm tot}_{\rm uni}$ is always greater than or equal to $\Psi^{\rm tot}$. Hence, for $\lambda \geq 1.007$, biaxial disclinated states are energetically preferred over both the uniaxial and the isotropic alternatives and, thus, represent energy minima.

6 Discussion

In contrast to the studies undertaken by Fried and Todres[1,2] and Fried, Korchagin and Todres,[2] we address the question of whether a nematic elastomeric material cross-linked in an isotropic state and subjected to an isochoric homogeneous deformation is capable of sustaining disclinations. In particular, we consider a cylindrical specimen with circular cross-section that is subjected to a deformation which transforms a generic cross-section of the undeformed specimen homogeneously into an ellipse while preserving area locally. Assuming that, when they exist, the directors are perpendicular and parallel to the level sets of the deformation, the theory developed by Fried, Korchagin and Todres[3] then yields a system of semilinear elliptic partial-differential equations for the asphericities. We use numerical methods to study those equations subject to variationally-natural boundary conditions. Our numerical results indicate that the specimen can exhibit states in which an isotropic tubular core with characteristic cross-section on the order of 10^{-2} μm is surrounded by an extra-core region in which the conformation is biaxial. Energetic considerations show that, for reasonable choices of

the material parameters, such biaxial disclinated states are preferred over both isotropic and uniaxial disclinated alternatives whenever the strain is greater than or equal to 0.7%. Thus, the theory predicts that an even relatively mild distortions are likely to induce dislinations in isotropically cross-linked nematic elastomers. Further, our results show that the mechanically-induced transition between the isotropic and biaxial nematic states in such a material is of second order.

References

1. Fried, E. & Todres, R. E. Prediction of disclinations in nematic elastomers. *Proc. Natl. Acad. Sciences USA* **98**, 14773–14777 (2001).
2. Fried, E. & Todres, R. E. Disclinated states in nematic elastomers. *J. Mech. Phys. Solids* **50**, 2691–2716 (2002).
3. Fried, E., Korchagin, V. & Todres, R. E. Biaxial disclinated states in nematic elastomers. *J. Chem. Phys.* **119**, (2003).
4. Warner, M., Blandon, P. & Terentjev, E. M. Soft elasticity—deformation without resistance in liquid crystal elastomers. *J. Physique II* **4**, 93–102 (1994).
5. Ericksen, J. L. Liquid-crystals with variable degree of orientation. *Arch. Rational Mech. Anal.* **113**, 97–120 (1991).
6. Haller, I. Elastic constants of the nematic liquid crystalline phase of p-Methoxybenzylidene-p-n-Butylaniline (MBBA). *J. Chem. Phys.* **57**, 1400–1405 (1972).
7. Bunning, J. D., Faber, T. E. & Sherell, P. L. The Frank constants of nematic 5CB at atmospheric pressure. *J. Physique* **42**, 1175–1182 (1981).
8. Bradshaw, M. J., Raynes, E. P., Bunning, J. D. & Faber, T. E. The Frank constants of some nematic liquid crystals. *J. Physique* **46**, 1513–1520 (1985).
9. Virga, E. G. *Variational Theories for Liquid Crystals* (Chapman & Hall, London, 1994).
10. Schmidtke, J. Stille, W. & Strobl, G. Static and dynamic light scattering of a nematic side-group polysiloxane. *Macromolecules* **33**, 2922–2928 (2000).
11. Warner, M. and Terentjev, E. M. Nematic elastomers–a new state of matter? *Prog. Polym. Sci.* **21**, 853–891 (1996).
12. Chandrasekhar, S. & Ranganath, G. S. The structure and energetics of defects in liquid crystals. *Adv. Phys.* **50**, 2691–2716 (2002).
13. Swarztrauber, P. N. & Sweet, R. A. Efficient Fortran subprograms for the solution of separable elliptic partial differential equations. *ACM Trans. Math. Software* **5**, 352–364 (1979).

List of Recent TAM Reports

No.	Authors	Title	Date
951	Vainchtein, D. L., and H. Aref	Morphological transition in compressible foam—*Physics of Fluids* **13**, 2152–2160 (2001)	July 2000
952	Chaïeb, S., E. Sato-Matsuo, and T. Tanaka	Shrinking-induced instabilities in gels	July 2000
953	Riahi, D. N., and A. T. Hsui	A theoretical investigation of high Rayleigh number convection in a nonuniform gravitational field—*International Journal of Pure and Applied Mathematics*, in press (2003)	Aug. 2000
954	Riahi, D. N.	Effects of centrifugal and Coriolis forces on a hydromagnetic chimney convection in a mushy layer—*Journal of Crystal Growth* **226**, 393–405 (2001)	Aug. 2000
955	Fried, E.	An elementary molecular-statistical basis for the Mooney and Rivlin–Saunders theories of rubber-elasticity—*Journal of the Mechanics and Physics of Solids* **50**, 571–582 (2002)	Sept. 2000
956	Phillips, W. R. C.	On an instability to Langmuir circulations and the role of Prandtl and Richardson numbers—*Journal of Fluid Mechanics* **442**, 335–358 (2001)	Sept. 2000
957	Chaïeb, S., and J. Sutin	Growth of myelin figures made of water soluble surfactant—Proceedings of the 1st Annual International IEEE–EMBS Conference on Microtechnologies in Medicine and Biology (October 2000, Lyon, France), 345–348	Oct. 2000
958	Christensen, K. T., and R. J. Adrian	Statistical evidence of hairpin vortex packets in wall turbulence—*Journal of Fluid Mechanics* **431**, 433–443 (2001)	Oct. 2000
959	Kuznetsov, I. R., and D. S. Stewart	Modeling the thermal expansion boundary layer during the combustion of energetic materials—*Combustion and Flame*, in press (2001)	Oct. 2000
960	Zhang, S., K. J. Hsia, and A. J. Pearlstein	Potential flow model of cavitation-induced interfacial fracture in a confined ductile layer—*Journal of the Mechanics and Physics of Solids*, **50**, 549–569 (2002)	Nov. 2000
961	Sharp, K. V., R. J. Adrian, J. G. Santiago, and J. I. Molho	Liquid flows in microchannels—Chapter 6 of *CRC Handbook of MEMS* (M. Gad-el-Hak, ed.) (2001)	Nov. 2000
962	Harris, J. G.	Rayleigh wave propagation in curved waveguides—*Wave Motion* **36**, 425–441 (2002)	Jan. 2001
963	Dong, F., A. T. Hsui, and D. N. Riahi	A stability analysis and some numerical computations for thermal convection with a variable buoyancy factor—*Journal of Theoretical and Applied Mechanics* **2**, 19–46 (2002)	Jan. 2001
964	Phillips, W. R. C.	Langmuir circulations beneath growing or decaying surface waves—*Journal of Fluid Mechanics* (submitted)	Jan. 2001
965	Bdzil, J. B., D. S. Stewart, and T. L. Jackson	Program burn algorithms based on detonation shock dynamics—*Journal of Computational Physics* (submitted)	Jan. 2001
966	Bagchi, P., and S. Balachandar	Linearly varying ambient flow past a sphere at finite Reynolds number: Part 2—Equation of motion—*Journal of Fluid Mechanics* **481**, 105–148 (2003) (with change in title)	Feb. 2001
967	Cermelli, P., and E. Fried	The evolution equation for a disclination in a nematic fluid—*Proceedings of the Royal Society A* **458**, 1–20 (2002)	Apr. 2001
968	Riahi, D. N.	Effects of rotation on convection in a porous layer during alloy solidification—Chapter 12 in *Transport Phenomena in Porous Media* (D. B. Ingham and I. Pop, eds.), 316–340 (2002)	Apr. 2001
969	Damljanovic, V., and R. L. Weaver	Elastic waves in cylindrical waveguides of arbitrary cross section—*Journal of Sound and Vibration* (submitted)	May 2001
970	Gioia, G., and A. M. Cuitiño	Two-phase densification of cohesive granular aggregates—*Physical Review Letters* **88**, 204302 (2002) (in extended form and with added co-authors S. Zheng and T. Uribe)	May 2001

List of Recent TAM Reports (cont'd)

No.	Authors	Title	Date
971	Subramanian, S. J., and P. Sofronis	Calculation of a constitutive potential for isostatic powder compaction—*International Journal of Mechanical Sciences* (submitted)	June 2001
972	Sofronis, P., and I. M. Robertson	Atomistic scale experimental observations and micromechanical/ continuum models for the effect of hydrogen on the mechanical behavior of metals—*Philosophical Magazine* (submitted)	June 2001
973	Pushkin, D. O., and H. Aref	Self-similarity theory of stationary coagulation—*Physics of Fluids* **14**, 694–703 (2002)	July 2001
974	Lian, L., and N. R. Sottos	Stress effects in ferroelectric thin films—*Journal of the Mechanics and Physics of Solids* (submitted)	Aug. 2001
975	Fried, E., and R. E. Todres	Prediction of disclinations in nematic elastomers—*Proceedings of the National Academy of Sciences* **98**, 14773–14777 (2001)	Aug. 2001
976	Fried, E., and V. A. Korchagin	Striping of nematic elastomers—*International Journal of Solids and Structures* **39**, 3451–3467 (2002)	Aug. 2001
977	Riahi, D. N.	On nonlinear convection in mushy layers: Part I. Oscillatory modes of convection—*Journal of Fluid Mechanics* **467**, 331–359 (2002)	Sept. 2001
978	Sofronis, P., I. M. Robertson, Y. Liang, D. F. Teter, and N. Aravas	Recent advances in the study of hydrogen embrittlement at the University of Illinois—Invited paper, Hydrogen–Corrosion Deformation Interactions (Sept. 16–21, 2001, Jackson Lake Lodge, Wyo.)	Sept. 2001
979	Fried, E., M. E. Gurtin, and K. Hutter	A void-based description of compaction and segregation in flowing granular materials—*Continuum Mechanics and Thermodynamics*, in press (2003)	Sept. 2001
980	Adrian, R. J., S. Balachandar, and Z.-C. Liu	Spanwise growth of vortex structure in wall turbulence—*Korean Society of Mechanical Engineers International Journal* **15**, 1741–1749 (2001)	Sept. 2001
981	Adrian, R. J.	Information and the study of turbulence and complex flow—*Japanese Society of Mechanical Engineers Journal B*, in press (2002)	Oct. 2001
982	Adrian, R. J., and Z.-C. Liu	Observation of vortex packets in direct numerical simulation of fully turbulent channel flow—*Journal of Visualization*, in press (2002)	Oct. 2001
983	Fried, E., and R. E. Todres	Disclinated states in nematic elastomers—*Journal of the Mechanics and Physics of Solids* **50**, 2691–2716 (2002)	Oct. 2001
984	Stewart, D. S.	Towards the miniaturization of explosive technology—Proceedings of the 23rd International Conference on Shock Waves (2001)	Oct. 2001
985	Kasimov, A. R., and Stewart, D. S.	Spinning instability of gaseous detonations—*Journal of Fluid Mechanics* (submitted)	Oct. 2001
986	Brown, E. N., N. R. Sottos, and S. R. White	Fracture testing of a self-healing polymer composite—*Experimental Mechanics* (submitted)	Nov. 2001
987	Phillips, W. R. C.	Langmuir circulations—*Surface Waves* (J. C. R. Hunt and S. Sajjadi, eds.), in press (2002)	Nov. 2001
988	Gioia, G., and F. A. Bombardelli	Scaling and similarity in rough channel flows—*Physical Review Letters* **88**, 014501 (2002)	Nov. 2001
989	Riahi, D. N.	On stationary and oscillatory modes of flow instabilities in a rotating porous layer during alloy solidification—*Journal of Porous Media* **6**, 1–11 (2003)	Nov. 2001
990	Okhuysen, B. S., and D. N. Riahi	Effect of Coriolis force on instabilities of liquid and mushy regions during alloy solidification—*Physics of Fluids* (submitted)	Dec. 2001
991	Christensen, K. T., and R. J. Adrian	Measurement of instantaneous Eulerian acceleration fields by particle-image accelerometry: Method and accuracy—*Experimental Fluids* (submitted)	Dec. 2001
992	Liu, M., and K. J. Hsia	Interfacial cracks between piezoelectric and elastic materials under in-plane electric loading—*Journal of the Mechanics and Physics of Solids* **51**, 921–944 (2003)	Dec. 2001
993	Panat, R. P., S. Zhang, and K. J. Hsia	Bond coat surface rumpling in thermal barrier coatings—*Acta Materialia* **51**, 239–249 (2003)	Jan. 2002

List of Recent TAM Reports (cont'd)

No.	*Authors*	*Title*	*Date*
994	Aref, H.	A transformation of the point vortex equations—*Physics of Fluids* **14**, 2395–2401 (2002)	Jan. 2002
995	Saif, M. T. A, S. Zhang, A. Haque, and K. J. Hsia	Effect of native Al_2O_3 on the elastic response of nanoscale aluminum films—*Acta Materialia* **50**, 2779–2786 (2002)	Jan. 2002
996	Fried, E., and M. E. Gurtin	A nonequilibrium theory of epitaxial growth that accounts for surface stress and surface diffusion—*Journal of the Mechanics and Physics of Solids* **51**, 487–517 (2003)	Jan. 2002
997	Aref, H.	The development of chaotic advection—*Physics of Fluids* **14**, 1315–1325 (2002); see also *Virtual Journal of Nanoscale Science and Technology*, 11 March 2002	Jan. 2002
998	Christensen, K. T., and R. J. Adrian	The velocity and acceleration signatures of small-scale vortices in turbulent channel flow—*Journal of Turbulence*, in press (2002)	Jan. 2002
999	Riahi, D. N.	Flow instabilities in a horizontal dendrite layer rotating about an inclined axis—*Journal of Porous Media*, in press (2003)	Feb. 2002
1000	Kessler, M. R., and S. R. White	Cure kinetics of ring-opening metathesis polymerization of dicyclopentadiene—*Journal of Polymer Science A* **40**, 2373–2383 (2002)	Feb. 2002
1001	Dolbow, J. E., E. Fried, and A. Q. Shen	Point defects in nematic gels: The case for hedgehogs—*Proceedings of the National Academy of Sciences* (submitted)	Feb. 2002
1002	Riahi, D. N.	Nonlinear steady convection in rotating mushy layers—*Journal of Fluid Mechanics* **485**, 279–306 (2003)	Mar. 2002
1003	Carlson, D. E., E. Fried, and S. Sellers	The totality of soft-states in a neo-classical nematic elastomer—*Journal of Elasticity*, in press (2003) with revised title	Mar. 2002
1004	Fried, E., and R. E. Todres	Normal-stress differences and the detection of disclinations in nematic elastomers—*Journal of Polymer Science B: Polymer Physics* **40**, 2098–2106 (2002)	June 2002
1005	Fried, E., and B. C. Roy	Gravity-induced segregation of cohesionless granular mixtures—*Lecture Notes in Mechanics*, in press (2002)	July 2002
1006	Tomkins, C. D., and R. J. Adrian	Spanwise structure and scale growth in turbulent boundary layers—*Journal of Fluid Mechanics* (submitted)	Aug. 2002
1007	Riahi, D. N.	On nonlinear convection in mushy layers: Part 2. Mixed oscillatory and stationary modes of convection—*Journal of Fluid Mechanics* (submitted)	Sept. 2002
1008	Aref, H., P. K. Newton, M. A. Stremler, T. Tokieda, and D. L. Vainchtein	Vortex crystals—*Advances in Applied Mathematics* **39**, in press (2002)	Oct. 2002
1009	Bagchi, P., and S. Balachandar	Effect of turbulence on the drag and lift of a particle—*Physics of Fluids*, in press (2003)	Oct. 2002
1010	Zhang, S., R. Panat, and K. J. Hsia	Influence of surface morphology on the adhesive strength of aluminum/epoxy interfaces—*Journal of Adhesion Science and Technology* **17**, 1685–1711 (2003)	Oct. 2002
1011	Carlson, D. E., E. Fried, and D. A. Tortorelli	On internal constraints in continuum mechanics—*Journal of Elasticity*, in press (2003)	Oct. 2002
1012	Boyland, P. L., M. A. Stremler, and H. Aref	Topological fluid mechanics of point vortex motions—*Physica D* **175**, 69–95 (2002)	Oct. 2002
1013	Bhattacharjee, P., and D. N. Riahi	Computational studies of the effect of rotation on convection during protein crystallization—*Journal of Crystal Growth* (submitted)	Feb. 2003
1014	Brown, E. N., M. R. Kessler, N. R. Sottos, and S. R. White	*In situ* poly(urea-formaldehyde) microencapsulation of dicyclopentadiene—*Journal of Microencapsulation* (submitted)	Feb. 2003

List of Recent TAM Reports (cont'd)

No.	*Authors*	*Title*	*Date*
1015	Brown, E. N., S. R. White, and N. R. Sottos	Microcapsule induced toughening in a self-healing polymer composite—*Journal of Materials Science* (submitted)	Feb. 2003
1016	Kuznetsov, I. R., and D. S. Stewart	Burning rate of energetic materials with thermal expansion—*Combustion and Flame* (submitted)	Mar. 2003
1017	Dolbow, J., E. Fried, and H. Ji	Chemically induced swelling of hydrogels—*Journal of the Mechanics and Physics of Solids*, in press (2003)	Mar. 2003
1018	Costello, G. A.	Mechanics of wire rope—Mordica Lecture, Interwire 2003, Wire Association International, Atlanta, Georgia, May 12, 2003	Mar. 2003
1019	Wang, J., N. R. Sottos, and R. L. Weaver	Thin film adhesion measurement by laser induced stress waves—*Journal of the Mechanics and Physics of Solids* (submitted)	Apr. 2003
1020	Bhattacharjee, P., and D. N. Riahi	Effect of rotation on surface tension driven flow during protein crystallization—*Microgravity Science and Technology*, in press (2003)	Apr. 2003
1021	Fried, E.	The configurational and standard force balances are not always statements of a single law—*Proceedings of the Royal Society* (submitted)	Apr. 2003
1022	Panat, R. P., and K. J. Hsia	Experimental investigation of the bond coat rumpling instability under isothermal and cyclic thermal histories in thermal barrier systems—*Proceedings of the Royal Society of London A*, in press (2003)	May 2003
1023	Fried, E., and M. E. Gurtin	A unified treatment of evolving interfaces accounting for small deformations and atomic transport: grain-boundaries, phase transitions, epitaxy—*Advances in Applied Mechanics*, in press (2003)	May 2003
1024	Dong, F., D. N. Riahi, and A. T. Hsui	On similarity waves in compacting media—*Horizons in Physics*, in press (2003)	May 2003
1025	Liu, M., and K. J. Hsia	Locking of electric field induced non-180° domain switching and phase transition in ferroelectric materials upon cyclic electric fatigue—*Applied Physics Letters*, in press (2003)	May 2003
1026	Liu, M., K. J. Hsia, and M. Sardela Jr.	In situ X-ray diffraction study of electric field induced domain switching and phase transition in PZT-5H—*Journal of the American Ceramics Society* (submitted)	May 2003
1027	Riahi, D. N.	On flow of binary alloys during crystal growth—*Recent Research Development in Crystal Growth*, in press (2003)	May 2003
1028	Riahi, D. N.	On fluid dynamics during crystallization—*Recent Research Development in Fluid Dynamics*, in press (2003)	July 2003
1029	Fried, E., V. Korchagin, and R. E. Todres	Biaxial disclinated states in nematic elastomers—*Journal of Chemical Physics*, to appear (2003)	July 2003
1030	Sharp, K. V., and R. J. Adrian	Transition from laminar to turbulent flow in liquid filled microtubes—*Physics of Fluids* (submitted)	July 2003
1031	Yoon, H. S., D. F. Hill, S. Balachandar, R. J. Adrian, and M. Y. Ha	Reynolds number scaling of flow in a Rushton turbine stirred tank: Part I—Mean flow, circular jet and tip vortex scaling—*Chemical Engineering Science* (submitted)	Aug. 2003
1032	Raju, R., S. Balachandar, D. F. Hill, and R. J. Adrian	Reynolds number scaling of flow in a Rushton turbine stirred tank: Part II—Eigen-decomposition of fluctuation—*Chemical Engineering Science* (submitted)	Aug. 2003
1033	Hill, K. M., G. Gioia, and V. V. Tota	Structure and kinematics in dense free-surface granular flow—*Physical Review Letters*, in press (2003)	Aug. 2003
1034	Fried, E., and S. Sellers	Free-energy density functions for nematic elastomers—*Journal of the Mechanics and Physics of Solids* (submitted)	Sept. 2003
1035	Kasimov, A. R., and D. S. Stewart	On the dynamics of self-sustained one-dimensional detonations: A numerical study in the shock-attached frame—*Physics of Fluids* (submitted)	Nov. 2003
1036	Fried, E., and B. C. Roy	Disclinations in a homogeneously deformed nematic elastomer—*Nature Materials* (submitted)	Nov. 2003